

Noncontact Capacitive Sensing-Based Locomotion Transition Recognition for Amputees With Robotic Transtibial Prostheses

Enhao Zheng, *Student Member, IEEE*, and Qining Wang, *Member, IEEE*

Abstract—Recent advancement of robotic transtibial prostheses can restore human ankle dynamics in different terrains. Automatic locomotion transitions of the prosthesis guarantee the amputee's safety and smooth motion. In this paper, we present a noncontact capacitive sensing-based approach for recognizing locomotion transitions of amputees with robotic transtibial prostheses. The proposed sensing system is designed with flexible printed circuit boards which solves the walking instability brought by our previous system when using robotic prosthesis and improves the recognition performance. Six transtibial amputees were recruited and performed tasks of ten locomotion transitions with the robotic prosthesis that we recently constructed. The capacitive sensing system was integrated on the prosthesis and worked in combination with on-prosthesis mechanical sensors. With the cascaded classification method, the proposed system achieved 95.8% average recognition accuracy by support vector machine (SVM) classifier and 94.9% accuracy by quadratic discriminant analysis (QDA) classifier. It could accurately recognize the upcoming locomotion modes from the stance phase of the transition steps. In addition, we proved that adding capacitance signals could significantly reduce recognition errors of the robotic prosthesis in locomotion transition tasks. Our study suggests that the fusion of capacitive sensing system and mechanical sensors is a promising alternative for controlling the robotic transtibial prosthesis.

Index Terms—Capacitive sensing, locomotion transition recognition, robotic prosthesis, transtibial amputees.

I. INTRODUCTION

TRANSTIBIAL amputation severely influences the quality of amputees' daily life, as the ambulation is limited by the limb loss. The human ankle joint is important in ambulation by changing quasi-stiffness characteristics at different speeds [1] and adjusting angle changes at different terrains to meet the gait requirements [2]. Passive prostheses can effectively mimic

a human ankle at level walking by using a spring-damper structure [1]. However, during ambulation with different terrains which requires motion transitions, the users have to make extra effort to keep the balance and it causes unnatural gait patterns [2], [3]. Recent developments in micro-controller controlled robotic prostheses have greatly expanded the functions of the passive ones [4]–[10]. The robotic prosthesis can better restore the functions of missing limb(s) by adjusting the impedance parameters at different gait phases and/or providing extra torques at powered plantar flexion period [8], [15]. It also has the ability to regulate dynamic parameters at different terrains [3]. Thus, amputees can accomplish more natural gaits during ambulation with less metabolic cost by using robotic prostheses.

Current main control strategies of robotic prostheses include gait pattern generators [4], the muscle-skeletal control method [6], finite-state control [7], and hierarchical control strategy [12]. Among all the control methods, ambulation on different terrains requires corresponding parameters [11], [12]. Therefore, automatic transition is necessary for smooth and safe human motions. In order to accomplish accurate automatic transitions with robotic prostheses, researchers attempt to recognize the upcoming locomotion modes (for example, level walking to stair ascending) relying on sensors (mechanical sensors or neural sensors) and machine learning algorithms. It is quite important since it provides judgment information of locomotion transitions to the subsequent prosthetic controllers. On this topic, there were a few studies solely relying on mechanical sensors [12]–[14] integrated on prostheses. A great many researchers studied neural signals, e.g., surface electromyograph (sEMG) signals, on the residual limb for locomotion transition recognition [15]–[18] and combined sEMG with on-prosthesis mechanical signals [19]–[22] to produce more accurate results. Some of the studies implemented their approaches on robotic transtibial prostheses. For example, in [15], transitions between level walking and stair descent were successfully identified by the volitional contractions of the residual limb. In [16], a proportional EMG control method was designed, and the amputee could control the push-offs during stair ambulation. In [21], the authors combined sEMG signals of four residual limb muscles with on-prosthesis mechanical signals, and a detailed investigation with eight locomotion transitions on five subjects was carried out.

However, the methods mentioned still have challenges in recognizing locomotion transitions for controlling the prosthesis. Purely relying on mechanical sensors cannot meet the

Manuscript received February 15, 2015; revised August 06, 2015; accepted February 07, 2016. Date of publication February 12, 2016; date of current version March 06, 2017. This work was supported by the 2011 R&D Project of the Beijing Disabled Persons' Federation, by the National Natural Science Foundation of China under Grant 61005082, Grant 61020106005, and Grant 61533001, by the Beijing Municipal Science and Technology Project under Project Z151100003715001, Project Z151100000915073, and by the Beijing Nova Program under Grant Z141101001814001. *Corresponding author: Qining Wang* (e-mail: qiningwang@pku.edu.cn).

The authors are with the Robotics Research Group, College of Engineering, Peking University, Beijing 100871, China, and Beijing Engineering Research Center of Intelligent Rehabilitation Engineering, Beijing 100871, China (e-mail: zhengenhao@pku.edu.cn).

Color versions of one or more of the figures in this paper are available online at <http://ieeexplore.ieee.org>.

Digital Object Identifier 10.1109/TNSRE.2016.2529581

requirements of clinical use [13], especially when safety is the most important factor for lower-limb motions. Adding sEMG signals could produce higher recognition accuracies [21] and longer prediction time [19] than only using mechanical sensors. But using sEMG sensors induced some practical problems [13], [23], [24]. First, in long-time applications, the muscle fatigue and the presence of sweat decreased the performance of EMG signal sampling, which further failed the recognition of locomotion transitions. Second, for lower-limb amputees, especially for transtibial amputees who have smaller and fewer muscles on residual limbs, sEMG signals may not exhibit enough human motion information if there is muscle loss or muscle atrophy. Third, sEMG signals rely on electrodes that firmly contact the residual limb. The long-time pressure on sensing spots may cause pressure sores on the residual limb, which seriously influence the amputees' ambulation. Recently, our group has developed a new capacitance-based sensing approach for steady locomotion mode recognition [24]–[26]. In [24], we proposed a noncontact capacitance sensing system (C-Sens) as an alternative to overcome the drawbacks of sEMG sensors in steady locomotion mode recognition on passive prostheses.

The contributions of this study can be listed as follows. First, we improved the noncontact capacitance sensing system including the electrodes and the measurement system. The newly designed system both overcame the drawbacks of sEMG systems and solved the problems of previous electrodes in locomotion transition tasks using robotic prosthesis. Second, we integrated capacitive sensing system with on-prosthesis mechanical sensors to gain more accurate motion transition recognition. Ten locomotion transitions and six locomotion modes were investigated on six transtibial amputees using robotic prosthesis. Third, we addressed problems in locomotion transition tasks aiming for future clinical use. We trained the amputees to perform transitions with either of their legs which had never been achieved before. It is an important issue in clinical use of a robotic prosthesis. With the cascaded classification method, the system produced comparable results compared to other related studies.

II. ROBOTIC TRANSTIBIAL PROSTHESIS

A. Robotic Prosthesis Prototype

The robotic transtibial prosthesis (PKU-RoboTPro) that we recently proposed [3], consists of mechanical structure, control circuits, sensors and battery [see Fig. 1(a)]. We used a 50 W dc brushless motor from Maxon (EC 45–50 W) as the core of the driving system and equipped it with a 5.8 : 1 reduction gearbox. The total weight of the proposed prosthesis (excluding the rechargeable Li-ion battery) is 1.3 kg. The average power consumption of the prosthesis during one gait cycle is around 3.5 W, and a 0.28 kg rechargeable Li-ion battery can sustain a duration of more than 12 hours or 20 000 steps.

There were two inertial measurement units (IMUs) on the shank and the foot, respectively [see Fig. 1(a)]. Each IMU included a tri-axis gyroscope and a tri-axis accelerometer. The gyroscope has a full-scale range of 2000°/s and a resolution

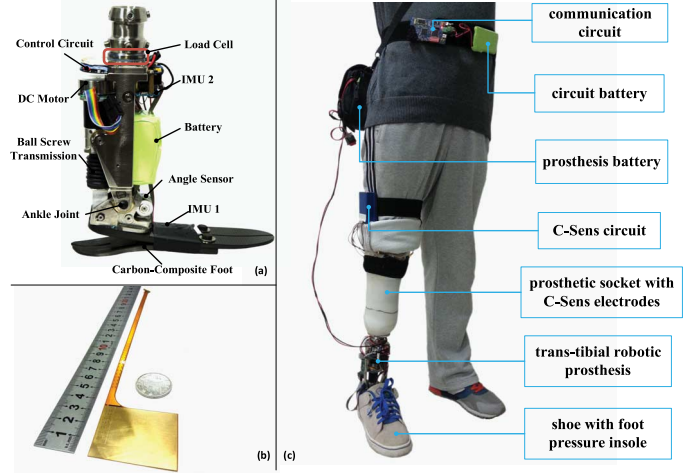


Fig. 1. (a) Structure of our designed robotic transtibial prosthesis (PKU-RoboTPro). The total weight of the prosthesis (excluding the battery) was 1.3 kg. (b) Electrodes of C-Sens. We built the C-Sens electrodes with flex printed circuit boards (Flex-PCB). The size of the electrode was 3.5 cm \times 4.5 cm. The length of one electrode was 24 cm. The thickness was 0.5 mm. (c) Placement of the system on an amputee. The C-Sens electrodes were fixed inside the prosthetic socket. The sensor data were transmitted to the computer via Bluetooth.

of 0.06°/s while the accelerometer had a full-scale range of 157 m/s² and a resolution of 0.005 m/s². A load cell (Interface LBS) was fixed on the leg to measure the interaction force between human body and the prosthesis. The single-axis load cell (Interface LBS) had a measurement range of 0–250 lbf. An absolute angle sensor (Angtron-RE-25) was used to record the ankle angle within the range from 25° dorsiflexion to 25° plantar flexion.

B. Implementation of Damping Control

We used a damping control method to control the prosthesis in the controlled flexion (CF) phase [3]. In ambulation, besides powered plantar (PP), CF [can be further divided into controlled plantar flexion (CP) and controlled dorsiflexion (CD)] is also important, since in CF, the ankle absorbs heel-strike shocks, stores energy, and provides proper resistance for smooth moving forward. The damping of the prosthetic ankle was controlled through changing the braking torque of the brushless dc motor. The braking torque τ_b was produced by the induced voltage when the stator windings of the brushless motor were shorted. Under this circumstance, τ_b was proportional to the motor speed n .

By switching on/off the motor-winding-short with a pulse width modulation (PWM) signal, the braking torque during the switch-on period became very large and the ankle joint could only rotate at a very low speed, while the braking torque during the switch-off period would be very small and the joint rotated quickly. With an appropriate on/off frequency, the braking torque was positively correlated with the duty cycle D of the PWM signal and the resulted equivalent braking torque τ_{eb} could be approximated as

$$\tau_{eb} = k_d D n. \quad (1)$$

As the duty cycle D determined the relationship between the torque and the speed, it could be regarded as the damping coefficient. k_d was the proportionality coefficient in the unit of Nm/rpm.

According to (1), the ankle impedance during CF was simplified as the damping coefficient D , and the control strategy became designing the damping-angle relationship. At the early stance, the ankle resistive torque was expected to be small to enable shock absorption and foot-flat. At the middle stance, the ankle torque was expected to increase to prevent the ankle from dorsiflexing too fast. When the ankle reached the maximal dorsiflexion, the ankle resistive torque was expected to be large enough to prevent the ankle from rotating. In this study, the damping-angle relationship was designed as the hyperbolic tangent function. The controller switched between the damping function of the CP (D_1) and the damping function of the CD (D_2) according to the angular rate $\dot{\theta}$, if $\dot{\theta} < 0$, $D = D_1$, else, $D = D_2$. The damping coefficients were calculated as

$$\begin{aligned} D_1 &= 1 - 0.5(\tanh(s_1(\theta - \theta_{d1})) + 1) \\ D_2 &= 0.5(\tanh(s_2(\theta - \theta_{d2})) + 1) \end{aligned} \quad (2)$$

where θ_{d1} was the threshold plantarflexion angle, θ was the current joint angle, s_1 was the sensitivity factor that decides the slope of the function and the resulting D_1 was the duty cycle of the PWM signal that controls the motor terminal short. θ_{d2} was the threshold dorsiflexion angle.

During the swing phase, we used the position control method to control the prosthesis moving back to the equilibrium angle. In different terrains such as ramps and stairs, we adjusted the coefficients to meet the dynamical requirements. Details of the control method applied in the robotic transtibial prosthesis can be found in [3].

III. C-SENS MEASUREMENT SYSTEM

In this study, we redesigned the capacitive sensing system for locomotion transition tasks using robotic prosthesis. The electrodes of the capacitive sensing system was designed with Flex-PCB [see Fig. 1(b)]. We integrated the electrode and the shielded connecting cable on the Flex-PCB circuit, which made the sensing front-ends much thinner (about 0.5-mm thickness) than the previous copper mesh-made electrodes [24]. The sensing method was still noncontact with human skin. The electrodes (Flex-PCB) were placed between the stump sock and the prosthetic socket, which measured the gap changes between the residual limb and the socket during locomotion (Fig. 2). We measured six spots on the residual limb with C-Sens. The sensing positions comprised the downside of the mid patella-tendon, the distal end of the residual tibia, the posterior of the distal end, the residual gastrocnemius muscle, the medial side of the thighbone (on the knee joint) and the lateral side of the thighbone (on the knee joint). The designed sampling circuit extracted C-Sens signals by measuring the capacitive charging time. A two-stage digital filter was implemented on the microcontroller unit (STMicroelectronics, Inc.) to remove the baseline shifting and the high frequency noises. The first stage filter was a second-order low-band-pass Butterworth filter

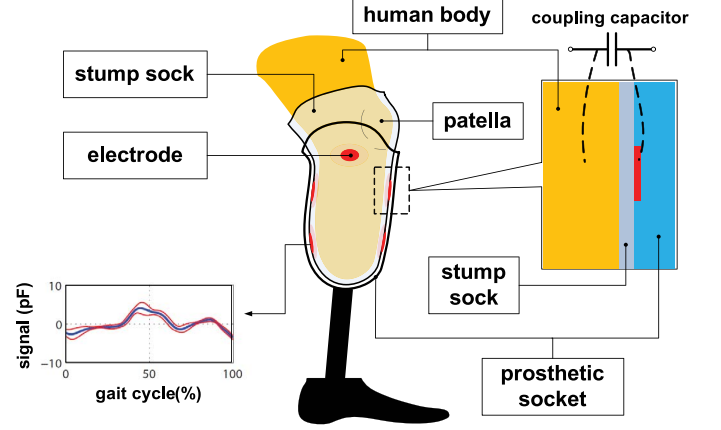


Fig. 2. Structure and the sensing principle of the sensing front-ends of the C-Sens. As shown in the figure, the transtibial prosthesis consists of the socket (usually made from rigid material) and the stump socks (usually made from silicon or rubber). The electrodes placed between the stump sock and the socket (red circles in the figure) and human body formed the coupling capacitors. The figure also shows the repeated-plotting signal of one gait cycle in level walking for channel six. The blue line is the average capacitance while the red lines are the standard deviation. Data were collected from TTA4.

(cut-off frequency 10 Hz). The second stage was the first-order dc notch filter (for the filtered signals see Fig. 2).

We also designed the sensing hardware and a graphic user interface, which enabled signal sampling in transition tasks and increased the efficiency of the training procedure using robotic prosthesis. In this study, more sensor data were sampled including six-channel capacitance signals, four-channel Euler angle signals (Pitch angle and Roll angle on the shank and on the foot of the prosthesis) and six-channel acceleration signals. The system preprocessed (two-stage filters for capacitance signals and limit filter for on-prosthesis sensors) and transmitted (all sensor data were wirelessly transmitted to the computer) the data packet in each 10 ms. We also designed a graphic user interface (GUI) on the computer to store the sensor data. The GUI received the data and presented real-time signal curves. The GUI gave visual feedback of the prosthetic signals (load cell signals, damping values, ankle angles) based on the preferences on the interface, which assisted the coefficients tuning procedure. The GUI reduced the time needed to get the subjects familiar with the robotic prosthesis. Besides C-Sens and on-prosthesis mechanical sensors, we placed a foot pressure insole in the amputated shoe to reaffirm the gait events detected by the loadcell. There were four force sensitive resistors (FSRs) on the insole to record the ground reaction forces during ambulation (for details see [27]).

IV. METHODS

A. Experimental Protocol

In this study, we employed six transtibial amputees who could finish the tasks in our experiment. All amputees were traumatic amputation. They could perform activities of daily living with their own passive prosthesis. They all used patella-tendon bearing prosthetic sockets for prostheses. Their activity level was similar to K-3 in U.S. k-ranking system. The demographic information of the subjects was shown in Table I. The residual

TABLE I
DETAILED INFORMATION FOR SIX SUBJECTS WITH TRANSTIBIAL AMPUTATION (TTA1-TTA6)

	Age	Weight(kg)	Height(cm)	Gender	Years post-amputation	Measured leg	Residual limb length ratio	Prosthesis for daily use
TTA1	55	75	176	M	18	L	36%	Teh Lin(SachFoot)
TTA2	29	72	172	M	7	R	36%	Teh Lin BKTQ042
TTA3	52	78	170	M	6	L	32%	Otto Bock 1C30
TTA4	45	71	170	M	8	L	40%	Otto Bock 1S90
TTA5	53	80	192	M	34	R	38%	Otto Bock 1S90
TTA6	31	65	172	M	6	L	31%	Teh Lin BK6060

limb length ratio was calculated as the ratio between the length of the residual shank (the distance between patella to the amputated site) and that of the sound shank (measured from patella to *malleolus lateralis*). We mounted their own prosthetic sockets on our robotic prosthesis with connectors. The electrodes of C-Sens were then fixed to the inner surface of the prosthetic socket. There was also a reference electrode inserted arbitrarily into the stump sock for circuit grounding. All subjects provided written and informed consent. The experiments were also approved by the Local Ethics Committee of Peking University.

We measured the data of six locomotion modes and ten locomotion transitions for all subjects. The locomotion modes we investigated included standing (St), walking (W), ramp ascending/descending (RA/RD), and stair ascending/descending (SA/SD). For locomotion transition investigation, we measured transitions between standing and walking ($St \Leftrightarrow W$, referred to as gait initiation and termination), ramp ascending/descending and walking ($RA/RD \Leftrightarrow W$), and stair ascending/descending and walking ($SA/SD \Leftrightarrow W$). The subjects were asked to perform the tasks at a particularly designed platform (Fig. 3). There was a four-step staircase (14-cm high and 40-cm depth) and a 2.5-m ramp (11.6-degree of inclination angle) on the platform. In our experiments, we investigated the transition data with different transitioning legs (the leg that first stepped onto the new terrain when there was a locomotion transition). We measured 15 groups of data for each transitioning leg for every subject. In each group, the subjects were asked to ambulate in two directions. As denoted in Fig. 3(a), in ambulation direction 1, the subjects started from standing to level walking, then upstairs and down the ramp. In this direction, $St \Rightarrow W$, $W \Rightarrow SA$, $SA \Rightarrow W$, $W \Rightarrow RD$, $RD \Rightarrow W$, and $W \Rightarrow St$ could be measured. The other five locomotion transitions were investigated in direction 2 [from right to the left in Fig. 3(a)]. We tuned the damping coefficients on every terrain for all the subjects based on their verbal feedback. Before the experiments, the subjects had a few hours to get familiar with the robotic prosthesis and experimental protocol. Then all subjects could learn how to perform a normal alternating leg pattern during stair ascending/descending and continually switch locomotion modes with either leg. During the experiment, the subjects were encouraged to ambulate with their favorite pace and speed. Based on their step length in initial trials, we pasted landmarks on the platform for transitioning leg instruction. We preset the walking cadences for the subjects to make the prosthesis automatically determine the current locomotion modes based on the step number. Therefore, we could automatically obtain the labeled data. There were handrails along

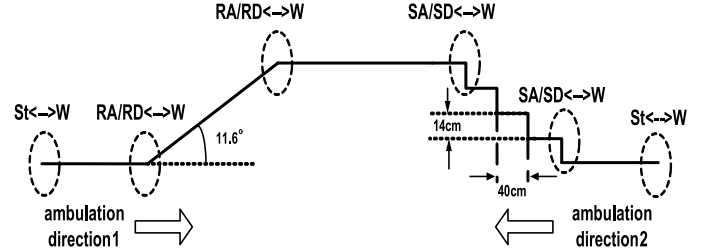


Fig. 3. Structure of the experiment platform. Ten locomotion transitions could be measured with two different ambulation directions in one group. The locomotion transitions were indicated in the figure.

the platform for safety. The subjects had a few minutes of rest between several groups (three or five) based on their request.

B. Data Segmentation and Labeling

In this study, we sampled six channels of C-Sens and the mechanical signals on the prosthesis, including three-axis acceleration and two-axis Euler angles (pitch angle and roll angle) of the shank and foot, respectively. The Euler angles were calculated on the microcontrollers of the prosthesis based on direction cosine matrix (DCM) method. All data were sampled at 100 Hz. We segmented the data stream into sliding windows, with the overlap of 10 ms (one sample period) [24]. The amputee can perform seamless transitions if the system successfully recognizes the locomotion modes before the critical gait event during ambulation. The gait phases in which transitions take place and the critical gait events are shown in Table II. For each locomotion transition, the first row presents the transition gait phase and gait events when the amputated leg performed the transition. While the second row shows that of the sound leg. Since there were no gait phases in gait initiation and gait termination, we did not show the transitions between standing (St) and walking (W). We automatically labeled the data of ambulation based on the critical gait event and gait phase in transitions. For training the first layer classification, we labeled the first second and the last second data of each trial as standing. We also manually reaffirmed the data of standing to insure there were no tendency of motion. The data between the first foot-off and the last foot-contact were labeled as ambulating.

C. Classification Method

In this study, we classified the locomotion transitions using the cascaded method. We firstly recognized standing and ambulation based on the data of C-Sens, then the data of ambulation were imported to another classification procedure. For the ambulation data, we used phase dependent classification

TABLE II
 LABELING OF LOCOMOTION TRANSITIONS

Locomotion modes	Gait phase in transition	Critical gait event
W \Rightarrow SA	swing \Rightarrow stance stance \Rightarrow swing	foot-contact on stair foot-off from level ground
W \Rightarrow SD	swing \Rightarrow stance stance \Rightarrow swing	foot-contact on stair foot-off from level ground
W \Rightarrow RA	swing \Rightarrow stance swing \Rightarrow stance	foot-contact on ramp foot-contact on ramp
W \Rightarrow RD	swing \Rightarrow stance swing \Rightarrow stance	foot-contact on ramp foot-contact on ramp
SA \Rightarrow W	swing \Rightarrow stance stance \Rightarrow swing	foot-contact on level ground foot-off from stair
SD \Rightarrow W	swing \Rightarrow stance stance \Rightarrow swing	foot-contact on level ground foot-off from stair
RA \Rightarrow W	swing \Rightarrow stance swing \Rightarrow stance	foot-contact on level ground foot-contact on level ground
RD \Rightarrow W	swing \Rightarrow stance swing \Rightarrow stance	foot-contact on level ground foot-contact on level ground

method, similar to our previous study [24]. Two classifiers were trained for the stance phase and the swing phase, respectively. The sliding window method (mentioned previously) was used to segment the data and calculate the feature sets. We used the signal of on-prosthesis loadcell to detect the gait events of foot-contact (FC) and foot-off (FO). A threshold was determined individually based on initial measurements. Before the experiment of each subject, we measured the signals of on-prosthesis loadcell when the participant's amputated leg rested freely above the ground for 10 seconds and stand still for 10 seconds. We averaged the loadcell data over 10 s of the two measurements. The threshold was calculated as

$$\text{Threshold} = \text{AVE}_{\text{rest}} + \frac{(\text{AVE}_{\text{stand}} - \text{AVE}_{\text{rest}})}{10} \quad (3)$$

where AVE_{rest} stands for the average value of data when the amputee's leg freely rested above the ground, while $\text{AVE}_{\text{stand}}$ is that of standing. The result was defined as the threshold to detect gait events. We rechecked the results after the experiments and found out that there were no misdetections.

D. Feature Set and Classifiers

We calculated several time-domain features on each sliding window for C-Sens signals and on-prosthesis mechanical signals. There were six features for C-Sens and four features for on-prosthesis mechanical sensors:

$$\begin{aligned} f_{c1} &= \text{avg}(X), f_{c2} = \text{std}(X), \\ f_{c3} &= \text{sum}(\text{abs}(\text{diff}(X))), \\ f_{c4} &= \text{max}(X), f_{c5} = \text{min}(X), f_{c6} = \text{sum}(\text{abs}(X)), \\ f_{m1} &= \text{avg}(X), f_{m2} = \text{std}(X), f_{m3} = \text{max}(X), \\ f_{m4} &= \text{sum}(X), \end{aligned}$$

where f_{ci} ($i = 1, 2, \dots, 6$) stands for the features of C-Sens, and f_{mi} ($i = 1, 2, 3, 4$) stands for the features of on-prosthesis mechanical sensors. X is the N -length data vector of one analysis window. $\text{avg}(X)$ and $\text{std}(X)$ are the average value of X

and the standard deviation of X , respectively. $\text{diff}(X)$ is the difference of X , which is a $(N - 1)$ -length vector and the i th element of $\text{diff}(X)$ is $X(i + 1) - X(i)$. $\text{sum}(X)$ is the summation of X . $\text{abs}(X)$ is the absolute value of X . The features concatenated a 76-dimension vector including 36 C-Sens features (six features and six channels) and 40 mechanical features (2 IMUs were implemented on the robotic prosthesis; in each IMU there were pitch angle, roll angle and three-axis accelerations).

In this study, we evaluated the performance of quadratic discriminant analysis (QDA) classifier, support vector machine (SVM) classifier (kernel based), linear support vector machine (linear-SVM) and logistic regression (LR). QDA estimated its classification parameters based on the multivariate normal (Gaussian) distribution model. It was proved to be effective in steady locomotion mode recognition [24]. It produced accurate results with a simple model and was also computationally efficient in real-time implementation. A kernel-based SVM classifier constructed an optimal hyperplane to separate the training data in high dimensional feature space via nonlinear kernel function. It was reported to perform better than LDA and artificial neural networks (ANN) in EMG-based human motion recognition [19], [28]. By comparison, the hyperplane of the linear-SVM was built in the original data space. The kernel function was the inner product. For the two SVM classifiers in this study, we used one-against-one (OAO) binary classification structure to fulfill multi-class classification. There were ten binary SVM classifiers for each gait phase of ambulation mode recognition. The C-support vector machine (C-SVC) was used as our SVM optimization model. The weight penalty method was also used to balance the training data. We chose polynomial function as the kernel function for the nonlinear SVM classification. For LR, we used softmax function [29] to deal with multi-classes. The discriminant function was expressed as

$$h(x^{(i)}) = \frac{1}{\sum_{\theta} e^{\theta_j^T x^{(i)}}} [e^{\theta_1^T x^{(i)}}, e^{\theta_2^T x^{(i)}}, \dots, e^{\theta_k^T x^{(i)}}]^T \quad (4)$$

where $\theta_1^T, \theta_2^T, \dots, \theta_k^T$ are the parameters of the model. $x^{(i)}$ is one sample of the data. The element that has the largest value in the result vector indicates the class. To obtain the parameters, the cost function is expressed as

$$\begin{aligned} J(\theta) &= -\frac{1}{m} \left[\sum_{i=1}^m \sum_{j=1}^k 1\{y^i = j\} \log \frac{e^{\theta_j^T x^{(i)}}}{\sum_{\theta} e^{\theta_j^T x^{(i)}}} \right] \\ &\quad + \frac{\lambda}{2} \sum_{i=1}^m \sum_{j=1}^k \theta_{ij}^2 \end{aligned} \quad (5)$$

where λ is the decay factor to make the cost function strictly convex. In our study, we used the limited memory Broyden-Fletcher-Goldfarb-Shanno (L-BFGS) method to optimize the parameters. The decay factor was set as 10^{-4} , and the maximum iteration number was 200 (the training procedure usually terminated at 150–180 iteration times).

E. Evaluation Method

In this study, N -fold cross-validation (LOOCV) were used for the training and testing of the classifiers. In this procedure, data of one fold were used as the testing set, and the remaining data were used as the training set. The process was repeated N times until all the folds were used for testing set. We used sliding windows to segment the data stream and recognize locomotion transitions. Thus, the overall recognition error (RE) was defined as

$$RE = \frac{N_{\text{mis}}}{N_{\text{total}}} \times 100\% \quad (6)$$

where N_{mis} is the number of misrecognized testing data and N_{total} is total number of testing data. We separately evaluated the gait initiation and termination and ambulation modes. For ambulation mode evaluation, we used a confusion matrix to better illustrate the recognition performance of certain locomotion modes. A detailed definition of a confusion matrix can be found in [24]. In this study, repeated measures analysis of variance (ANOVA) and pair t-test were conducted for analyses of the recognition errors. The significance level was 0.05 ($\alpha = 0.05$). In one-way ANOVA, the independent factor was sliding window length and the dependent factor was the average recognition error rate. In two-way ANOVA, the independent factors were classifiers and sliding window length, while the dependent factor was the average recognition error rate.

V. RESULTS

A. Classification of Standing and Ambulation

In this study, we used a cascaded classification method, in which we firstly classified the data into standing and ambulation, then we made another classification on ambulation data to recognize other locomotion modes. Compared with classification locomotion modes, distinguishing standing and ambulation was much easier. We utilized the data of C-Sens and on-prosthesis mechanical sensors (excluding loadcell signals). With initial tests, we picked out $\text{avg}(X) + \text{std}(X) + \max(X) + \min(X)$ as C-Sens feature set and $\text{avg}(X) + \text{std}(X)$ for mechanical sensor feature set. We used QDA classifier and 250-ms sliding window length for classification. For all the subjects, we could accurately (100% recognition accuracy) recognize the ambulation from the first FO to the last FC. Note that the classifier also successfully recognized the procedure of gait initiation and termination (representative results of one trial in Fig. 4). Therefore, we utilized the ambulation data classified by the first layer of classifier for subsequent analysis.

B. Classifiers and Sliding Window Length

The recognition performance was influenced by the classifiers and the sliding window length (Fig. 5). Statistical analysis demonstrated that there were significant effects of classifiers on average recognition errors ($F(1.14, 5.71) = 15.88$, $p = .007$, Greenhouse-Geisser correction, two-way repeated measures ANOVA). Among the four classifiers, softmax (LR) produced the highest recognition errors while SVM (kernel-based) produced the lowest (see Fig. 5). Linear-SVM and QDA

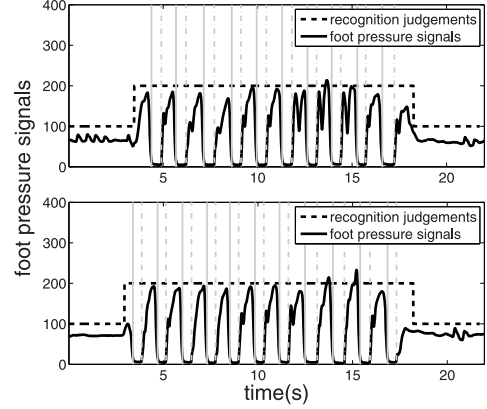


Fig. 4. Representative pseudo results of recognition between standing and ambulation. The data were collected from the first trial of TTA6. Two ambulation cadences are shown. The dashed horizontal lines denote the summation of foot pressure insole signals as the reference. The dotted horizontal lines denote the recognition judgements. The gray vertical lines show the gait events of foot-contact (dashed line) and foot-off (dotted line).

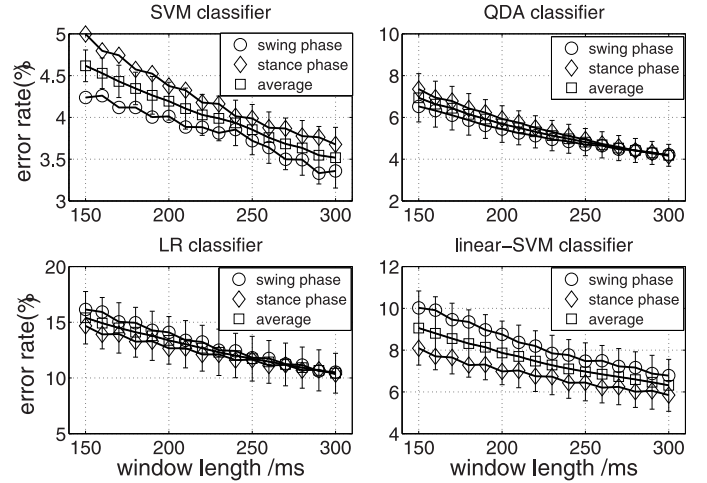


Fig. 5. Recognition performance with sliding window length changing from 150 to 300 ms. Subfigures show the recognition performance using SVM classifier, QDA classifier, LR classifier and linear-SVM classifier, respectively. The results of the swing phase (circles) and the stance phase (diamond shape) are shown. The average errors of the two phases are shown as the squares. Data are averaged across the six subjects; error bars represent average \pm SEM.

performed comparably well, but Linear-SVM required much longer time for training. Therefore, we selected SVM (kernel based) and QDA for the subsequent classification. In order to test the influence of the sliding window length, we conducted one-way repeated measure ANOVA. There were significant effects of sliding window length on average recognition errors for both SVM ($F(1.13, 5.64) = 14.59$, $p = .009$, Greenhouse-Geisser correction) and QDA ($F(1.01, 5.05) = 13.20$, $p = .015$, Greenhouse-Geisser correction). We then compared the recognition error rates of 300-ms window length (lowest error rate) with that of other window lengths by pair t-test. For SVM, the difference of the average recognition errors became insignificant when the sliding window length was larger than 270 ms. The critical window length was 240 ms for the swing phase and 230 ms for the stance phase (although not consistent), respectively. For QDA, there were no clear trends indicating the recognition errors settled, as all the average errors were significantly

TABLE III
CONFUSION MATRIX (MEAN) FOR SIX AMPUTEES WITH SVM CLASSIFIER(%)

Gait phase	Targets	Estimation modes				
		W	SA	SD	RA	RD
swing	W	95.9	0.2	0.1	2.3	1.5
	SA	1.1	97.9	0.1	0.8	0.1
	SD	1.4	0.3	97.1	0.2	1.1
	RA	5.7	0.6	0.1	93.6	0.1
	RD	4.9	0.0	0.5	0.1	94.5
stance	W	93.2	4.2	2.0	0.2	0.4
	SA	4.2	94.4	0.7	0.4	0.3
	SD	4.2	1.0	94.1	0.1	0.6
	RA	0.8	0.4	0.1	98.7	0.0
	RD	1.3	0.1	0.1	0.0	98.5

TABLE IV
CONFUSION MATRIX (MEAN) FOR SIX AMPUTEES WITH QDA CLASSIFIER(%)

Gait phase	Targets	Estimation modes				
		W	SA	SD	RA	RD
swing	W	92.9	0.2	0.4	3.6	2.9
	SA	0.7	97.9	0.3	1.0	0.7
	SD	0.4	0.0	99.2	0.1	0.2
	RA	7.8	0.6	0.1	91.4	0.1
	RD	5.1	0.1	1.7	0.1	93.0
stance	W	92.4	3.4	3.0	0.7	0.4
	SA	4.5	94.2	0.3	0.9	0.1
	SD	6.8	0.7	92.1	0.0	0.4
	RA	1.5	0.1	0.0	98.3	0.0
	RD	1.8	0.1	0.6	0.0	97.6

higher than that of the 300-ms window. We therefore selected the optimal window length based on SVM. For SVM, the statistical analysis revealed that the errors settled from 230 to 270 ms. Larger window length leads to lower recognition error rates, but longer response time and larger computational loads. By trading off between these factors, we took 250 ms as a compromising window length for the subsequent analysis.

C. Overall Recognition Accuracy

The overall recognition accuracies of every locomotion mode are shown in Tables III and IV. We calculated the recognition results with SVM classifier and QDA classifier. The results of the 15-fold LOOCV were presented. We observed from the recognition accuracies that SVM produced slightly better results than QDA classifier (95.8% average accuracy versus 94.9% average accuracy). For both classifiers, swing phase and the stance phase yielded the same average accuracies. But recognition results of the specific locomotion modes were different between gait phases and showed similar trends for the two classifiers. During the swing phase, ambulation on stairs (SA/SD) could be more accurately recognized than ambulating on ramps (RA/RD), but the results of the stance phase were quite the opposite. Among all the locomotion modes, the lowest recognition accuracy took place in stair descending of QDA classifier (92.1%).

We also evaluated the influence of the transitioning legs to overall recognition performance. The average accuracies dropped at least 5% for both QDA and SVM, if the data of only one transitioning leg were trained. Therefore, training with both transitioning legs was indispensable to obtain satisfactory recognition results.

D. Contributions of C-Sens to Recognition Performance

We firstly calculated recognition performance with C-Sens signals and on-prosthesis mechanical signals separately. The classification parameters were the same as those mentioned previously (15-fold LOOCV, 250-ms sliding window length). Both transitioning legs were taken into consideration. Results showed that on-prosthesis mechanical sensors could provide more accurate recognition results than C-Sens signals for continuous ambulation (except TTA6). Using C-Sens signals alone produced 32.3% average error rate with QDA classifier and 45.4% error rate with SVM classifier. C-Sens signals could not replace on-prosthesis mechanical sensors in locomotion transition recognition, but combining C-Sens signals could significantly reduce recognition error compared with purely using on-prosthesis mechanical sensors. The fusion of C-Sens and mechanical sensors yielded the lowest error rate.

We conducted a pair t-test on average recognition error rates to test the statistical significance. Adding capacitance signals could produce lower error rates than purely using mechanical sensors for all the locomotion modes ($t(5) = -4.89, p = .005$ for SVM; $t(5) = -15.17, p = .001$ for QDA, pair t-test). We also compared the recognition results in details to analyze the contribution of C-Sens to recognition results using robotic transtibial prosthesis (Fig. 6). The capacitive sensing system could provide more enhancements on SA/SD for SVM. In the swing phase of SD, $t(5) = -3.18, p = .025$, and in the stance phase of SA, $t(5) = -4.65, p = .006$. For QDA, the capacitive sensing system significantly reduced the error rate in W ($t(5) = -4.46, p = .007$ in the swing phase; $t(5) = -3.44, p = .018$ in the stance phase), SD ($t(5) = -4.35, p = .007$ in the swing phase; $t(5) = -5.13, p = .004$ in the stance phase) and RA ($t(5) = -2.63, p = .047$ in the stance phase). Although no statistical evidence, the improvement on W in the stance phase of SVM and SA of QDA was obvious, in which C-Sens reduced the error rate by 30% to 50%. The results proved that in locomotion transition recognition tasks using robotic transtibial prosthesis, where accuracy was crucial for safety, the fusion of C-Sens and mechanical sensors were necessary to obtain the highest recognition accuracy.

E. Analysis of Pseudo-Real-Time Recognition

We evaluated pseudo-real-time results to analyze the recognition performance more precisely. Most recognition errors occurred near the critical gait events (Fig. 7). The recognition parameters were the same as those mentioned before (250-ms window length, 15-fold LOOCV). Both transitioning legs were taken into consideration. For each subject, we selected the better classifier for classification. From TTA1 to TTA5 we chose SVM for classification and for TTA6 we chose QDA. In this study, ninth-order majority voting was used to remove the random errors in the raw results, which was shown as the blue lines in Fig. 7. We checked the results of all subjects. The recognition judgments quickly reached the correct values during transitions between level walking and stair ascending/descending, while there were more errors in transitions between ramps and level walking.

We then calculated the majority voting results for the three gait phases: Pre-FC (9 judgments), Post-FC (9 judgments) and

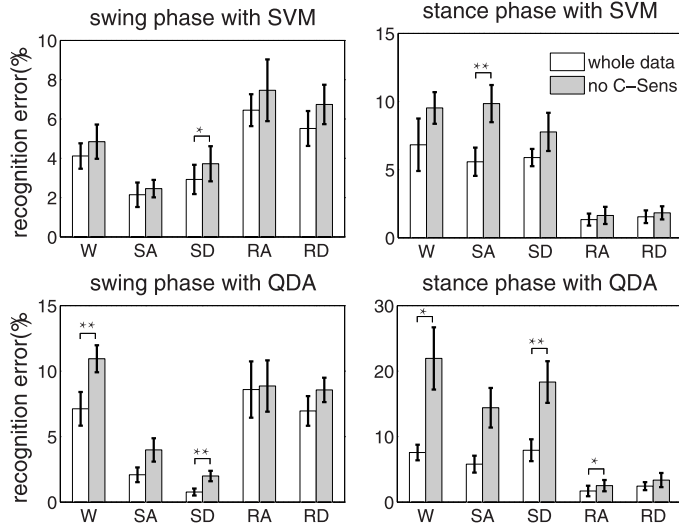


Fig. 6. Comparison of the recognition results between using C-Sens plus mechanical sensors and using purely mechanical sensors. The horizontal axis shows the abbreviations of the locomotion modes. The white bars represent recognition errors of using C-Sens and mechanical sensors, while the gray ones show the results of excluding C-Sens signals. Error bars stand for \pm SEM. Data are averaged across six subjects. * represents $p < 0.05$; ** represents $p < 0.01$.

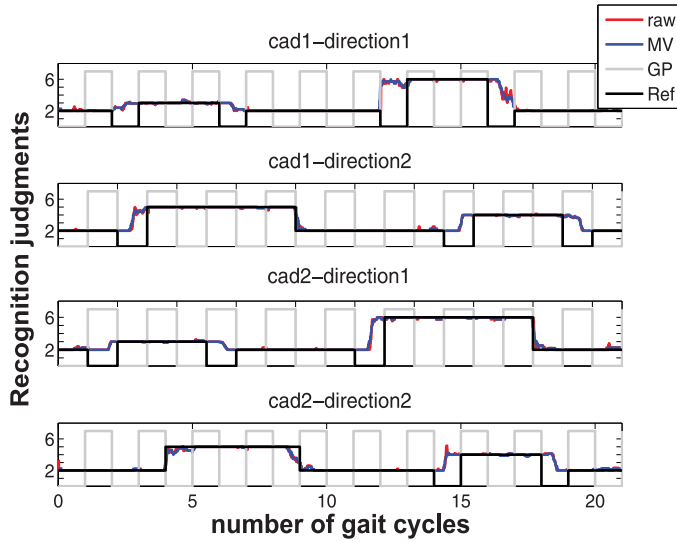


Fig. 7. Pseudo-real-time recognition results of TTA3. The horizontal axis shows the normalized gait cycles. The vertical axis denotes the recognition judgments, where 2 represents level walking, 3 represents stair ascending, 4 represents stair descending, 5 represents ramp ascending and 6 represents ramp descending. The raw recognition results (raw), results with majority voting (MV), reference locomotion modes (Ref), and gait phases (GP) are shown in different colors. The titles of the subfigures show the results of ambulation cadences. The recognition judgments normalized in one gait phase were averaged across all the trials.

Pre-FO (15 judgments). We summed up the number of steps which were different from the reference motion labels (see Table V). There were 60 steps in each column of the table. We observed from the results that almost all the recognition judgments could reach correct values during the stance phase of the transition steps. For the results of Pre-FO, all subjects excluding TTA1 could successfully recognize all the transition

TABLE V
MAJORITY VOTING OF RECOGNITION JUDGMENTS FOR THREE GAIT PHASES

Gait phase	Subjects	Locomotion transitions			
		W \leftrightarrow SA	W \leftrightarrow SD	W \leftrightarrow RA	W \leftrightarrow RD
Pre-FC	TTA1	2(1)	4(2)	5	11
	TTA2	3(2)	2	9(1)	4(1)
	TTA3	1	1	4(2)	4
	TTA4	2(2)	7(2)	7(1)	7(1)
	TTA5	6(5)	9(5)	10	15
	TTA6	0	3(2)	4	13(3)
Post-FC	TTA1	5(1)	5(1)	8	7
	TTA2	2(1)	2	10(2)	3(1)
	TTA3	0	0	1	7
	TTA4	4	7(1)	10(5)	4(1)
	TTA5	3(1)	3(3)	2	8
	TTA6	0	1(1)	2	10(2)
Pre-FO	TTA1	0	2	0	0
	TTA2	0	0	0	0
	TTA3	0	0	0	0
	TTA4	0	0	0	0
	TTA5	0	0	0	0
	TTA6	0	0	0	0

steps. Most of the errors occurred at the foot-contact of the transition steps when the amputated leg performed the transitions (see the error steps of PreFC and PostFC). There were more error steps in transitions between level walking and ambulation on ramps when the amputated leg performed the transition. A substantial part of errors were due to confusions between RA/RD and SA/SD (number of steps is shown in the brackets). The rest of the error steps were misclassified to the locomotion modes before the transition.

VI. DISCUSSION

The proposed noncontact capacitive sensing method is promising as an EMG-alternative in the control of the robotic prosthesis. It overcame the drawbacks of EMG-based sensing systems and meanwhile produced comparable recognition performance. The studies of [15] and [16] showed promising results of direct EMG-based control, but the performances were limited. The EMG signals generated by the volitional contractions acted as a trigger for binary mode control (level walking and stair descending [15]; push-off and no push-off [16]). No systematic locomotion experiments on multisubjects were conducted to validate the effectiveness. In [21], the system produced about 95% average accuracy across three discrete analysis windows, by fusing the information of EMG signals and mechanical signals. By comparison, our noncontact sensing strategy produced comparable results (95.8% accuracy) for six locomotion modes and ten locomotion transitions. In our study, the amputees performed transitions with either of their legs, which were more difficult tasks than [21]. Thus, our designed capacitive sensing strategy produced comparable results with sEMG-based systems and at the same time freed human skin from contacting with electrodes.

In this study, we made great improvements compared with our previous work [24]. First, the newly designed capacitance electrodes (Flex-PCB based) solved the problems of our previous ones in locomotion transition tasks using robotic prosthesis. The electrodes were as thin as 0.5 mm, which increased the fitness inside the prosthetic socket. The copper mesh-made electrodes had a thickness of 1 mm and produced

satisfactory steady mode recognition results on passive prostheses. However, the 1-mm thick sensing front-ends negatively affected the ambulation when using a robotic prosthesis. In our initial tests for locomotion transition recognition using robotic prosthesis, we employed TTA4 and used the copper mesh-made electrodes. During the experiment, the subject stated that the robotic prosthesis was not stable enough on his leg after the electrodes were placed inside. Since the robotic prosthesis was heavier than the passive one, the slight influence caused by the electrodes increased the risks of dropping. We then calculated the results using the collected data (the subject was TTA4 and all the transitions with both legs were included) with copper mesh-made electrodes and compared them with the results of using Flex-PCB ones. The control parameters (damping coefficients and load-cell thresholds) and the classification schemes (QDA and SVM, 250-ms window length, 15-fold LOOCV and feature set) were all the same. QDA produced 73.1% accuracy at swing phase and 72.8% accuracy at the stance phase, while SVM produced 78.8% accuracy and 77.8% accuracy at the swing phase and the stance phase, respectively. The accuracies were much lower than that of using Flex-PCB electrodes for TTA4 (QDA: swing phase 93.8%, stance phase 95.2%; and SVM: swing phase 94.7%, stance phase 96.8%). Besides, all subjects reported there were no uncomfortable feelings during the ambulation. Second, in this study, we addressed the problems in locomotion transition tasks using robotic prosthesis. Our previous study focused on the evaluation of the capacitive sensing system, and the tasks were steady locomotion modes with passive prostheses. By comparison, in this study, the locomotion transition tasks were performed with either leg with a robotic prosthesis, which had never been achieved before by the amputees. With cascaded classification and a postprocessing method, the system produced satisfactory results which could be used as reference in future clinical use.

Recognition accuracy was crucial for the safety of the lower-limb prosthesis control. The recognition results of this study indicated that on-prosthesis mechanical sensors mainly contributed to the recognition performance (over 90% recognition accuracy), which was in conformity with the related studies [13], [14]. However, the recognition performance was directly linked to ambulation safety. Any reduction of the recognition errors could further reduce the risks of fall and injury. C-Sens could significantly ($p < 0.01$) reduce the average error rates made by mechanical sensors. The error reduction made by capacitive sensing system was more effective in level walking, stair ascending and stair descending (Fig. 6).

We observed from pseudo-real-time results that for transitions between W and SA/SD, most of the transitions were successfully recognized at the critical gait event of the transition step. We also found that almost half of the error steps in $W \Leftrightarrow SA/SD$ were confused with $W \Leftrightarrow RA/RD$ (as was shown by the numbers in the brackets of Table V). If excluding ramps, the system could produce more accurate recognition judgments. However, the misclassifications between W and RA/RD were more than that of SA/SD. Most errors occurred in transitions of $RD \Leftrightarrow W$ and $W \Leftrightarrow RA$ when the amputated side performed the transition. There are two possible reasons based on our *post hoc* analysis. First, $RA \Rightarrow W$ and $SA \Rightarrow W$ showed similar gait

patterns during the swing phase, where both locomotion modes required amputees to drag the foot upwards to the level ground. The damping coefficients of the robotic prosthesis were similar between these two locomotion modes. The case was similar in $RD \Rightarrow W$ and $SD \Rightarrow W$. Second, in $W \Rightarrow RD$, we observed the subjects placed most of their body weight on the sound leg which was still on the ground. It made the gait patterns more similar to level walking at the PreFC and PostFO, which caused the delay. The case was similar in $W \Rightarrow RA$. Actually in our experiments, the damping coefficients of the easily confused transitions also showed similar values. In future clinical use, the error near FC will change the damping curve of CP phase. But, it will not cause sudden changes on ankle stiffness or motion directions. The safety of the amputees can still be insured.

There are several limitations in this study. First, there were no quantitative metrics as a measure to tune the prosthetic damping coefficients on different terrains. Before the experiments, we set the damping control coefficients based on the verbal feedback of the amputees. However, the subjects have become accustomed to their passive prostheses for years. Although all the amputees finished our tasks after a few hours of training, quantitative metrics were still needed for reliable use. Second, although we improved C-Sens signal quality by newly designed electrodes. It was still limited by the materials of the stump sock which acted as the dielectric of the coupling capacitors. The more elastic the stump sock, the more information C-Sens could convey. Among all the subjects, TTA3 and TTA6 used silicon-made socks while TTA1 and TTA5 used hard materials. This difference in stump socks was reflected in recognition performance. TTA3 and TTA6 produced lower error rates than TTA1 and TTA5 in recognition results.

Future work will be done in the following aspects. First, quantitative metrics on gait patterns like gait symmetry will be exploited to evaluate the effectiveness of the damping coefficients. In future experiments, we will tune the prosthetic parameters based on the objective metrics. Second, experiments on real-time control of the robotic prosthesis will be carried out. The practical problems in real-time control, especially the problems of ramp ambulation, will be addressed. Third, further attempts will be made on developing custom prosthetic socket embedded with C-Sens electrodes. Moreover, we will explore the potentials of C-Sens for volitional control. It is worth exploring whether the amputee can volitionally generate a particular signal pattern in some certain locomotion modes.

VII. CONCLUSION

In this study, we have implemented the noncontact capacitive sensing system C-Sens on our designed robotic transtibial prosthesis for locomotion transition recognition. The C-Sens sensing system was redesigned solving the problems of our previous system in locomotion transition tasks using robotic prostheses. Six locomotion modes and ten locomotion transitions were investigated on six subjects. Moreover, transitions with either leg were taken into consideration. The integration of C-Sens on robotic prostheses could significantly reduce the recognition errors. With our selected classification strategies, our system produced comparable recognition performance with sEMG-mechanical fusion-based studies. We also verified that data of both

transitioning legs should be trained for reliable recognition. We believe the fusion of C-Sens with mechanical sensors can be a good alternative to sEMG-mechanical fusion for controlling robotic transtibial prosthesis. Future endeavors will be focused on real-time control of robotic prosthesis and validating the performance of the proposed system in clinical applications.

ACKNOWLEDGMENT

The authors would like to thank the anonymous reviewers for their valuable suggestions that improved this paper. They would also like to thank Q. Zhu and J. Li for their contributions in the experiments.

REFERENCES

- [1] A. H. Hansen, D. S. Childress, S. C. Miff, S. A. Gard, and K. P. Mesplay, "The human ankle during walking: Implications for design of biomimetic ankle prostheses," *J. Biomech.*, vol. 37, no. 10, pp. 1467–1474, 2004.
- [2] D. H. Gates, "Characterizing ankle function during stair ascent, descent, and level walking for ankle prosthesis and orthosis design," Master's, Dept. Biomed. Eng., Boston Univ., Boston, MA, USA, 2004.
- [3] Q. Wang, K. Yuan, J. Zhu, and L. Wang, "Walk the walk: A lightweight active transtibial prosthesis," *IEEE Robot. Automat. Mag.*, vol. 22, no. 4, pp. 80–89, Apr. 2015.
- [4] R. Jimenez-Fabian and O. Verlinden, "Review of control algorithms for robotic ankle systems in lower-limb orthoses, prostheses, and exoskeletons," *Med. Eng. Phys.*, vol. 34, no. 4, pp. 397–408, 2012.
- [5] J. Hitt, T. Sugar, M. Holgate, R. Bellman, and K. Hollander, "Robotic transtibial prosthesis with biomechanical energy regeneration," *Ind. Robot.*, vol. 36, no. 5, pp. 441–447, 2009.
- [6] M. F. Eilenberg, H. Geyer, and H. Herr, "Control of a powered ankle-foot prosthesis based on a neuromuscular model," *IEEE Trans. Neural Syst. Rehabil. Eng.*, vol. 18, no. 2, pp. 164–173, Mar. 2010.
- [7] S. K. Au, J. Weber, and H. Herr, "Powered ankle-foot prosthesis to reduce metabolic consumption," *IEEE Trans. Robot.*, vol. 25, no. 1, pp. 51–66, Feb. 2009.
- [8] P. Cherelle, V. Grosu, A. Matthys, B. Vanderborght, and D. Lefeber, "Design and validation of the ankle mimicking prosthetic (AMP-) foot 2.0," *IEEE Trans. Neural Syst. Rehabil. Eng.*, vol. 22, no. 1, pp. 138–148, Jan. 2014.
- [9] A. H. Shultz, J. E. Mitchell, D. Truex, B. E. Lawso, and M. Goldfarb, "Preliminary evaluation of a walking controller for a powered ankle prosthesis," in *Proc. Int. Conf. Robotics and Automation*, 2013, pp. 4838–4843.
- [10] J. Zhu, Q. Wang, and L. Wang, "On the design of a powered transtibial prosthesis with stiffness adaptable ankle and toe joints," *IEEE Trans. Ind. Electron.*, vol. 61, no. 9, pp. 4797–4807, Sep. 2014.
- [11] L. Fradet, M. Alimusaj, F. Braatz, and S. I. Wolf, "Biomechanical analysis of ramp ambulation of transtibial amputees with an adaptive ankle foot system," *Gait Posture*, vol. 32, pp. 191–198, 2010.
- [12] H. A. Varol, F. Sup, and M. Goldfarb, "Multiclass real-time intent recognition of a powered lower limb prosthesis," *IEEE Trans. Biomed. Eng.*, vol. 57, no. 3, pp. 542–551, Mar. 2010.
- [13] A. J. Young, A. M. Simon, and L. J. Hargrove, "A training method for locomotion mode prediction using powered lower limb prostheses," *IEEE Trans. Neural Syst. Rehabil. Eng.*, vol. 22, no. 3, pp. 671–677, May 2014.
- [14] A. J. Young, A. M. Simon, N. P. Fey, and L. J. Hargrove, "Intent recognition in a powered lower limb prosthesis using time history information," *Ann. Biomed. Eng.*, vol. 42, no. 3, pp. 631–641, 2014.
- [15] S. Au, M. Berniker, and H. Herr, "Powered ankle-foot prosthesis to assist level-ground and stair-descent gaits," *Neural Netw.*, vol. 21, no. 4, pp. 654–666, 2008.
- [16] O. Kannape and H. Herr, "Volitional control of ankle plantar flexion in a powered transtibial prosthesis during stair-ambulation," in *Proc. IEEE 35th Annu. Int. Conf. IEEE Engineering in Medicine and Biology Soc.*, 2008, pp. 1662–1665.
- [17] H. Huang, T. A. Kuiken, and R. D. Lipschutz, "A strategy for identifying locomotion modes using surface electromyography," *IEEE Trans. Biomed. Eng.*, vol. 56, no. 1, pp. 65–73, Jan. 2009.
- [18] L. J. Hargrove, A. M. Simon, A. J. Young, R. D. Lipschutz, S. B. Finucane, D. G. Smith, and T. A. Kuiken, "Robotic leg control with EMG decoding in an amputee with nerve transfers," *N. Engl. J. Med.*, vol. 369, no. 24, pp. 2364–2364, 2013.
- [19] H. Huang, F. Zhang, L. Hargrove, Z. Dou, D. R. Rogers, and K. B. Englehart, "Continuous locomotion-mode identification for prosthetic legs based on neuromuscular-mechanical fusion," *IEEE Trans. Biomed. Eng.*, vol. 58, no. 10, pp. 2867–2875, Oct. 2011.
- [20] L. Du, F. Zhang, M. Liu, and H. Huang, "Toward design of an environment-aware adaptive locomotion-mode-recognition system," *IEEE Trans. Biomed. Eng.*, vol. 59, no. 10, pp. 2716–2725, Oct. 2012.
- [21] D. C. Tkach and L. J. Hargrove, "Neuromechanical sensor fusion yields highest accuracies in predicting ambulation mode transitions for transtibial amputees," in *Proc. IEEE 35th Annu. Int. Conf. IEEE Engineering in Medicine and Biology Soc.*, 2013, pp. 3074–3077.
- [22] B. Chen, Q. Wang, and L. Wang, "Adaptive slope walking with a robotic transtibial prosthesis based on volitional EMG control," *IEEE/ASME Trans. Mechatronics*, vol. 20, no. 5, pp. 2146–2157, May 2015.
- [23] J. W. Sensinger, B. A. Lock, and T. A. Kuiken, "Adaptive pattern recognition of myoelectric signals: Exploration of conceptual framework and practical algorithms," *IEEE Trans. Neural Syst. Rehabil. Eng.*, vol. 17, no. 3, pp. 270–278, May 2009.
- [24] E. Zheng, L. Wang, K. Wei, and Q. Wang, "A noncontact capacitive sensing system for recognizing locomotion modes of transtibial amputees," *IEEE Trans. Biomed. Eng.*, vol. 61, no. 9, pp. 2911–2920, Sep. 2014.
- [25] E. Zheng, B. Chen, K. Wei, and Q. Wang, "Lower limb wearable capacitive sensing and its applications to recognizing human gaits," *Sensors*, vol. 13, no. 10, pp. 13334–13355, 2013.
- [26] B. Chen, E. Zheng, X. Fan, T. Liang, Q. Wang, K. Wei, and L. Wang, "Locomotion mode classification using a wearable capacitive sensing system," *IEEE Trans. Neural Syst. Rehabil. Eng.*, vol. 21, no. 5, pp. 744–755, Sep. 2013.
- [27] X. Wang, Q. Wang, E. Zheng, K. Wei, and L. Wang, "A wearable plantar pressure measurement system: Design specifications and first experiments with an amputee," in *Proc. 12th Int. Conf. Intelligent Autonomous Systems*, 2012, pp. 273–281.
- [28] M. A. Oskoei and H. Hu, "Support vector machine-based classification scheme for myoelectric control applied to upper limb," *IEEE Trans. Biomed. Eng.*, vol. 55, no. 8, pp. 1956–1965, Aug. 2008.
- [29] E. R. Ziegel, "The elements of statistical learning," *Technometrics*, pp. 267–268, 2003.



Enhao Zheng (S'13) received the B.Sc. degree in automatic control from Xidian University (Xi'an), China, in 2010. He is currently working towards the Ph.D. degree under the supervision of Prof. Qining Wang in the Robotics Research Group, College of Engineering, Peking University, Beijing, China.

His research interests include human motion detection, capacitive sensing and human-machine interface.



Qining Wang (S'06–M'09) received the B.Sc. degree in computer science and technology from China University of Geosciences, Beijing, China, in 2004, and the Ph.D. degree in dynamics and control from Peking University, Beijing, China, in 2009.

He was an Assistant Professor in the Center for Systems and Control, College of Engineering, Peking University, from July 2009 to July 2012. He is currently an Associate Professor in the College of Engineering, Peking University, and the Director of the Beijing Engineering Research Center of Intelligent Rehabilitation Engineering. He is the Project Leader of the robotic prosthesis R&D group, Peking University. He has been author/coauthor of more than 100 scientific papers in international journals and refereed conference proceedings and of 21 national and international patents. His research interests are in the fields of bio-inspired robots and rehabilitation robotics.